Fusion Engineering and Design 151 (2020) 111357

Contents lists available at ScienceDirect

Fusion Engineering and Design

journal homepage: www.elsevier.com/locate/fusengdes

Status of the DEMO blanket attachment system and remaining challenges

Z. Vizvary[a,*], M.L. Richiusa[a], C. Bachmann[b], I.A. Maione[c], C. Vorpahl[b]

[a] CCFE, Culham Science Centre, Abingdon, Oxon, OX14 3DB, UK
[b] EUROfusion – Programme Management Unit, Boltzmannstrasse 2, 85748, Garching, Germany
[c] Karlsruhe Institute of Technology (KIT), Hermann-von-Helmholtz-Platz 1, 76344, Eggenstein-Leopoldshafen, Germany

ARTICLE INFO

Keywords:
DEMO
Blanket attachment concept
FEM

ABSTRACT

The DEMO blanket attachment concept is challenging due to several factors: the harsh radiation environment, the thermal expansion, the electro-magnetic loads, the remote maintenance feasibility, and the accurate control of the alignment of the breeding blanket first wall during operation. There are two inboard and three outboard blanket segments per vacuum vessel sector to be installed and extracted by remotely controlled tools through a single upper vertical port. The design of the fixations of the blanket segments to the VV complies with the strategy to avoid the need for front side access for engagement and release. The attachment system has been designed for the numerous critical load cases, including normal operation, dwell between pulses, plasma disruptions, fast discharge of the magnet coils, and accidental conditions such as loss of blanket coolant. At the same time the attachments must guarantee the stresses in the blanket segments not to exceed limits.

This paper introduces the attachment concept and describes the finite element model that has been built to assess the blanket attachment system. The model represents one sector of the DEMO machine. The results focus on the reaction forces transmitted at individual attachment locations to define these interfaces and guide the design of the individual supports.

1. Introduction

The blanket attachment system has to cope with various loading conditions: Gravity, thermal expansion, static magnetic forces during operation on the ferritic steel of the in-vessel components (IVCs), electro-magnetic forces during central disruptions (major disruption, MD),vertical displacement events (VDE) and toroidal field coil fast discharge (TFCFD), and loss of coolant accidents (LOCA).

The principle approach of the integration of in-vessel components in DEMO is based on avoiding the need for engagement/release of mechanical supports, pipe connections or electrical straps from the front and through the first wall (FW). This is to avoid remote maintenance (RM) tools operating on a regular basis in the very high gamma radiation environment in the plasma chamber. The basic blanket attachment concept is introduced in [1].

The blanket attachment concept has been assessed regarding the structural behaviour of the breeding blanket (BB) segments to the critical loads. To this end a shell element-based finite element (FE) model was used of one sector of the DEMO vacuum vessel (VV) with the associated five BB segments. The deformation of the BB segments and the reaction forces transmitted through their individual supports are presented in this article.

2. Attachment system description

2.1. Basic concept

The attachment system needs to support the blanket against very large electromagnetic (EM) loads, in particular radial forces as well as moments about the radial axis. At the same time the supports need to allow for the significant thermal deformation of the blanket, which reaches locally more than 500 °C in operation, and must maintain at the same time good alignment of the FW; charged particles following the, mainly toroidal, magnetic field lines would otherwise cause excessive local incident heat loads [2]. The choice was therefore made to support the blankets at the bottom *and* on the top, see Fig. 1. This choice allows also reducing and better controlling the displacements of the feeding pipe interfaces on the blanket backside. This concept however does not allow for free blanket thermal expansion and it is essential to verify that reaction forces on its vertical supports do not become excessive in any condition. The accidental loss of active blanket cooling is expected the worst scenario in this respect.

In addition to radial/vertical supports each blanket segment has toroidal shear keys that engage into corresponding slots in the VV. These shear keys react the large radial moments acting on the blanket

* Corresponding author.
E-mail address: zsolt.vizvary@ukaea.uk (Z. Vizvary).

https://doi.org/10.1016/j.fusengdes.2019.111357
Received 27 July 2019; Received in revised form 17 September 2019; Accepted 1 October 2019
Available online 02 December 2019

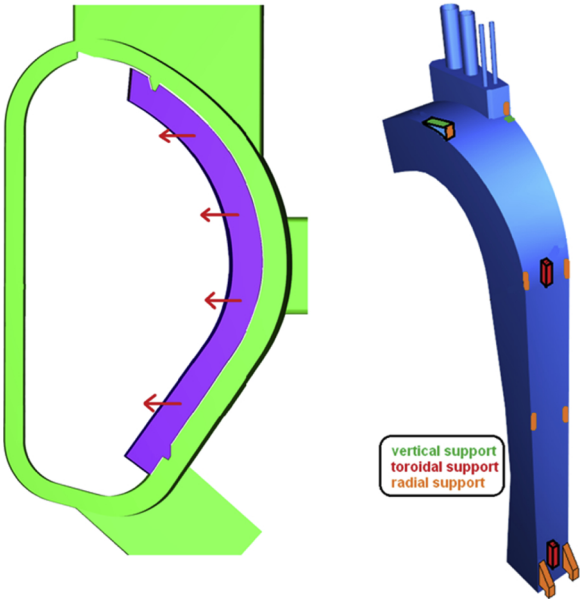

Fig. 1. Left: Radial and vertical supports of the BB vertical segments and quasi-static ferromagnetic forces (red arrows), right: Toroidal shear keys of the inboard segment (red). (For interpretation of the references to colour in this figure legend, the reader is referred to the web version of this article).

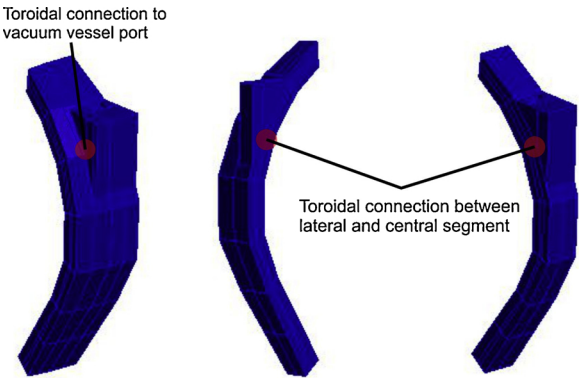

Fig. 2. Toroidal support locations between the VV and lateral segments and the COB and lateral segments (exploded view).

during a fast plasma current quench that occurs during a disruption. The inboard segments have two shear keys, one at the bottom and one at the top, providing a statically determined support condition (Fig. 1). The outboard segments were found too long and flexible for only two toroidal shear keys to suffice. Hence a third toroidal support has been implemented at the outboard side of the upper port (Fig. 2).

The blanket and its attachments have to be compatible with RM requirements. The first disengagement movement should e.g. progressively increase the gap between support and BB to avoid locking/jamming. Sliding movements should be avoided to prevent seizing and damage. The envisaged blanket removal kinematics is shown on Fig. 3. In addition, to reduce the actions required by RH tools bolts, pins or other locking components requiring release prior to blanket removal were avoided. Instead we rely on the large and constant radial ferromagnetic force acting on the ferritic blanket steel to induce a preload pushing the blanket against its supports closing assembly gaps and providing electrical contact. Electrical straps to guarantee electrical contact between blankets and VV are therefore not required. Temporary supports will likely be required during maintenance fixing in particular the inboard blankets to the upper port.

The simplicity of the individual blanket supports and the absences of bolts or other locking mechanisms do not allow individual position

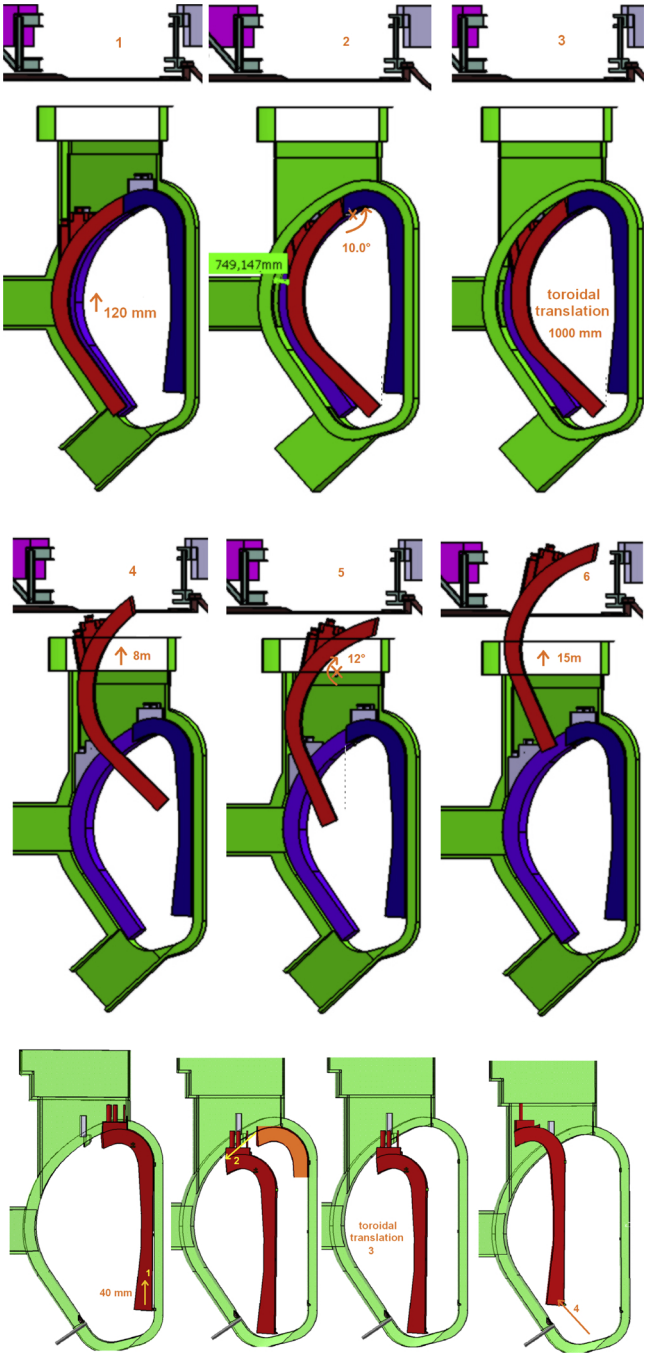

Fig. 3. Blanket kinematics.

control as possible in the attachment concept of the ITER blanket [3]. To ensure radial alignment of the FW the support pads on the backside of the BB segments can be custom-machined to compensate misalignments of the VV supports due to VV fabrication and assembly tolerances. Imperfections of the inboard blanket causing radial deviations of the inboard blanket poloidal shape will be corrected to some degree by the ferromagnetic radial force “bending the blanket straight”. Manufacturing imperfections of the outboard blanket poloidal shape cannot be corrected. The presence of plasma limiters on the outboard is however expected to reduce the alignment requirements of the FW on the outboard. The assessment of the effective alignment tolerances of the BB FW to be expected in different locations is yet incomplete.

2.2. Blanket supports inside upper port

Inside the upper port the blankets cannot be supported on the VV inner shell, instead they need to be supported on the inside of the port wall and by the port plugs, which are inserted into the port after the installation of the blankets is complete. Three port plugs are envisaged in each upper port, see Fig. 5. In some of the upper ports the central port plug will include a plasma limiter replacing the upper part of the central outboard segment (COB). The COB in these sectors will therefore be shorter and will be supported vertically and radially by the central port plug [3].

2.3. Inboard blanket supports

The inboard blanket is located on the high field side where the toroidal field is as high as $\sim 7-8$ T causing very large EM forces due to induced currents. Furthermore, the toroidal circumference on the inboard is smaller compared to the outboard. This causes increased current densities in case of poloidal currents that occur in the blanket either due to a TFCFD or due to vertical displacement events (VDEs) [4]. These poloidal currents cause vertically distributed large radial forces on the inboard blanket that act simultaneously with the ferromagnetic forces. Radial supports have been defined at four vertical levels and on both lateral sides of the inboard blankets providing support also against vertical moments. The vertical levels were chosen carefully based on FE analyses in order to minimize bending stresses in the BB and to avoid uneven load distribution to the different supports, see results.

3. FE model

The model includes one sector of the VV and the corresponding five blanket segments. It uses shell elements to reduce the degrees of freedom; it therefore adequately simulates the stiffness and therefore deformation of the components; local stress results are however unreliable.

The structural material of the BB is Eurofer 97. The blanket segments have internal shells representing the back-supporting structure (BSS), the manifold and the stiffening plates in the breeding zone (Fig. 4). This representation is considered to adequately represent the stiffness of both BB concept, i.e. the Helium-Cooled Pebble Bed (HCPB) and the Water-Cooled Lithium Lead (WCLL) designs [5,6]. The Eurofer density was modified such that the entire mass of the BB is accounted for. The model can be setup both as single-module segment (SMS) and multi-module segment (MMS), the latter by de-activating the elements linking the modules together.

Nonlinear springs were implemented in the model at each blanket support to allow studying the impact of assembly gaps. In particular, the vertical assembly gaps on the top supports need to be chosen carefully. During maintenance when the blanket is cold assembly gaps

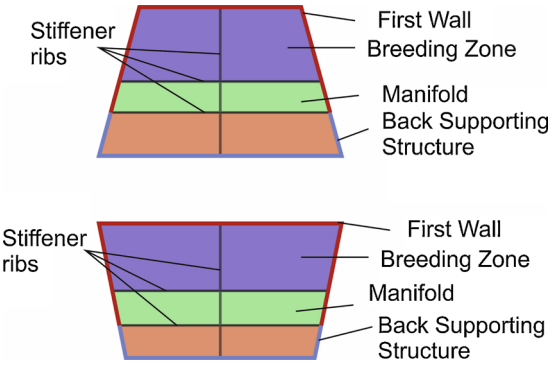

Fig. 4. Blanket segment cross-section in the FE model (top: outboard BB, bottom: inboard BB).

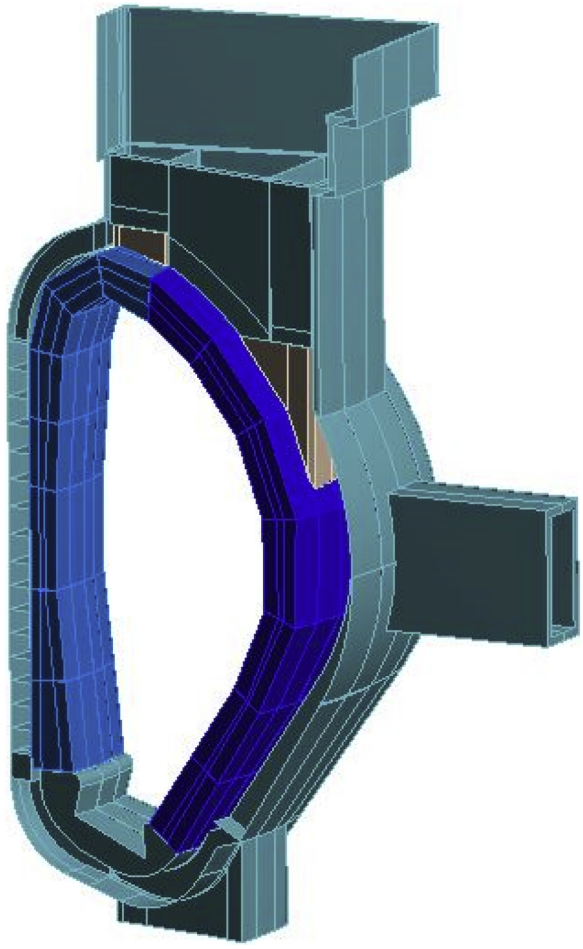

Fig. 5. FE model of VV sector and three upper port shield plugs (cyan) and five blanket segments (blue) with pipe connection locations "chimneys" (brown). (For interpretation of the references to colour in this figure legend, the reader is referred to the web version of this article).

are required. In addition, some of the thermal expansion difference between the BB segments and the VV needs to be free to avoid excessive vertical forces on the supports. At the same time during operation the blanket needs to be in contact with its VV supports on the top in order to ensure the location of the FW in the upper part of the blanket.

The upper port configuration [7] with three shield plugs split has been implemented (Fig. 5).

The implemented gaps at the support locations (Fig. 6) are shown in Table 1. The location of the top central outboard segment is further down and radially outer compared to the lateral segments. It is foreseen that limiters may have to be installed in some of the upper ports and hence the central limiter will be shorter. In this study only the support location has been moved, the length of the segment is unaffected, and the loads are also not scaled yet for a shorter central segment with the aim of pursuing a uniform solution, if possible, for all the central outboard segments.

4. Loads

4.1. Single load cases

4.1.1. Dead weight

Inboard segments are assumed to weigh 60 tons, outboard segments to weigh 85 tons.

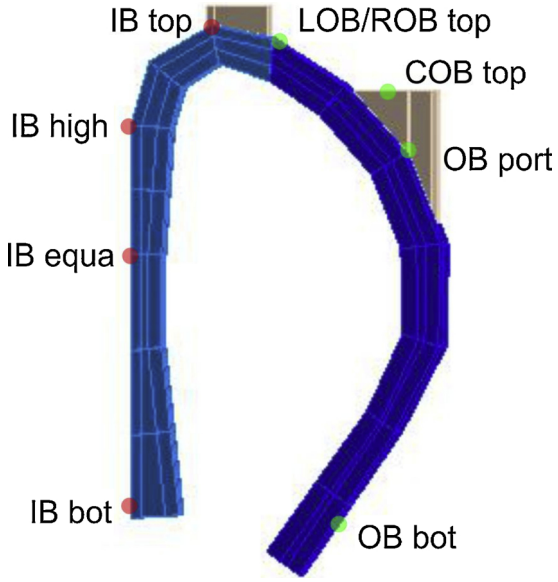

Fig. 6. Blanket attachment locations.

Table 1
Implemented gaps [mm].

BB support	Radial	Toroidal	Vertical
IB bot	± 3	± 1	0
IB equa	5	–	–
IB high	5	± 1	–
IB top	5	–	70
OB bot	± 3	± 1	0
LOB/ROB top	0	4	131
COB top	0	–	101
OB port left/right	–	4	–

4.1.2. Thermal conditions

The BB operating temperature regime has so far been defined only preliminarily as a radial variation along the blanket thickness (Fig. 8). The BB plasma-facing surface is at 527 °C, the back is at 300 °C (linear distribution applied). The operational temperature of the VV and the upper port the shield plugs is considered as 40 °C. Although the divertor operating temperature is defined higher it has been set to 40 °C in the model. This is not expected however to affect the results of the BB attachment system.

Ex-vessel LOCA is an important load case since the cooling of the BB is assumed to be inactive while the plasma remains being active for some time leading to a progressive temperature rise and consequent thermal expansion of the blanket segments. It is assumed that in case of an ex-vessel LOCA a soft plasma shutdown is triggered within 3 s, which causes the plasma fusion power to reduce to zero within 120 s [8]. The temperature distribution in the BB during an ex-vessel LOCA is given in [8] as a function of the distance from the plasma facing side, the highest temperatures occurring within the first few seconds of the event. We have therefore considered here the temperature predicted after 3 s in the FW (700 °C), which is a more conservative value than 585 °C also suggested in [8].

4.1.3. Ferromagnetic forces

The static ferromagnetic forces on the BB segments have been estimated based on an EM analysis of a previous DEMO configuration [9,10].

4.1.4. TF coil fast discharge (TFCFD) and VDEs

The DEMO VV load specification [11] defines the forces on the blankets during a TFCFD and four VDE cases. A magnet fast discharge event is triggered typically to protect the magnets from overheating by rapidly bringing their currents to zero with a time constant of 35 s. This generates a substantial poloidal current in the vacuum vessel and the in-vessel components (Fig. 7).

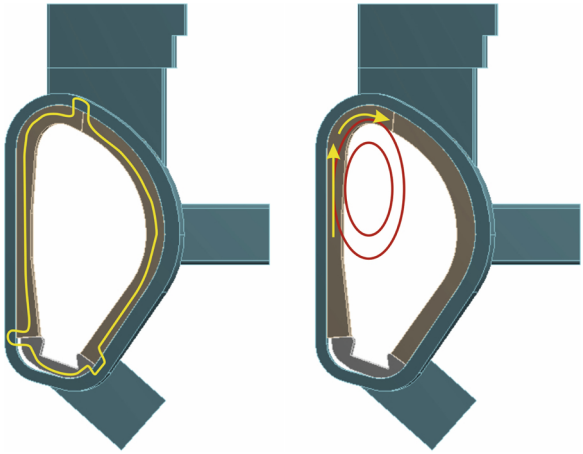

Fig. 7. Poloidal currents (yellow) in IVCs: induced during TFCFD (left), halo currents in upward VDE (right). (For interpretation of the references to colour in this figure legend, the reader is referred to the web version of this article).

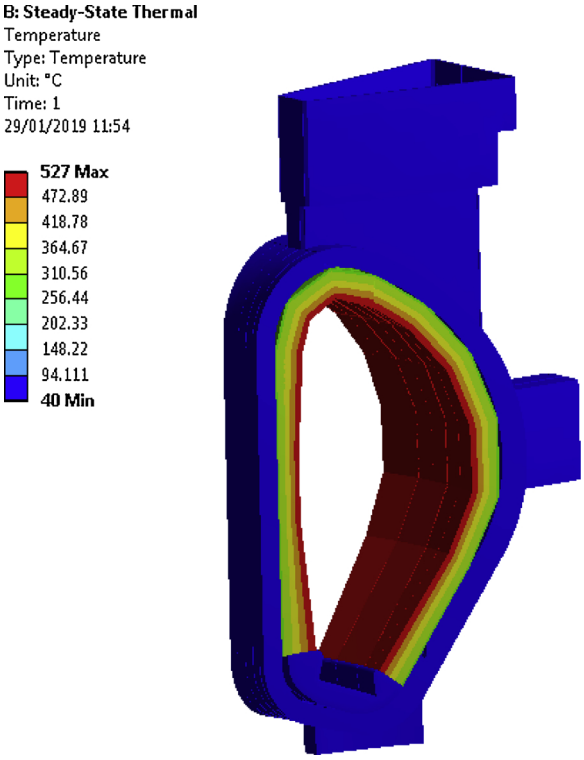

Fig. 8. Implemented temperature distribution for normal operation.

Similarly, due to VDEs, when the plasma touches the segments, poloidal currents (halo currents) will be present in the blanket segments (Fig. 7). These are highest in slow VDEs [4].

4.1.5. Major disruption

This load case refers to a central plasma disruption with the fastest current quench specified for DEMO: 77 ms [4]. Fast VDEs, which have the same current quench time, are not considered as it is assumed that the induced currents are similar to the major disruption case. The EM loads were calculated for the previous 2015 DEMO baseline [9,10]. The referenced calculations include only the current quench phase of the

Table 2
Main net loads on BB segments in different load cases, [MN, MNm]. Positive radial direction is pointing away from the machine centre, positive vertical direction is upwards.

Load case	Inboard BB			Outboard BB		
	F_{rad}	F_{vert}	M_{rad}	F_{rad}	F_{vert}	M_{rad}
Dead weight + ferromagn. force	−7.7	−0.6	0	−7.0	−0.9	0
TFCFD	−8.5	0.0	0	2.7	0.0	0
VDE slow up	−4.0	3.0	0	1.4	0.8	0
Major disruption	0	0	−9	0	0	17

disruption, hence toroidal magnetic field change is not considered. In this paper the moment values have been rounded up and the net forces have been omitted as they are at least an order of magnitude lower than the ferromagnetic forces. In the case of major central plasma disruption, the ferromagnetic forces are also considered (as all the magnets are on). Table 2 provides the most dominant net loads acting on the BB segments, which act along three degrees of freedom (DOF). Net loads occur also along the other 3 DOF but of less critical magnitude.

As the EM loads originally have been calculated for the 2015 baseline model which has different poloidal segmentation in this paper the total loads have been uniformly distributed to the BB segments.

4.2. Load combinations

Several static analyses have been performed for this purpose since dynamic amplification of BB segments is expected to be negligible [12].

- Normal operation (operational temperature + gravity + ferromagnetic forces)
- Ex-VV LOCA affecting both the inboard and the outboard BB segments (accidental temperature + gravity + ferromagnetic forces)
- TFCFD (operational temperature + gravity + ferromagnetic forces + TFCFD loads)
- VDE slow up (operational temperature + gravity + ferromagnetic forces + EM loads due to halo currents)
- TFCFD + VDE slow up (operational temperature + gravity + ferromagnetic forces + TFCFD loads + EM loads due to halo currents)
- Major disruption (operational temperature distribution + gravity + ferromagnetic forces + EM loads due to eddy currents)

5. Results

5.1. Reaction forces

In this section the occurring reaction forces in the most severe load scenarios are presented.

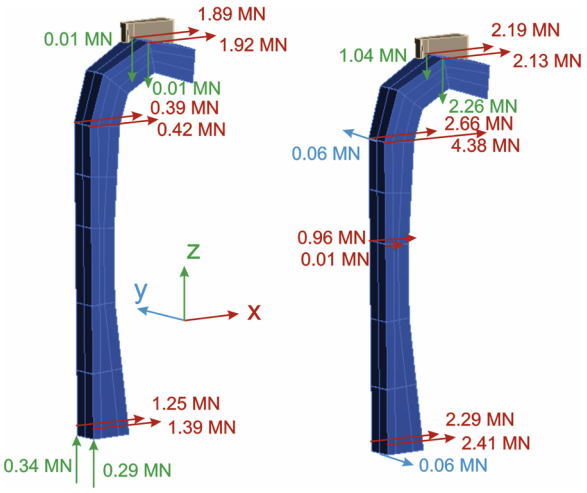

Fig. 9. Reaction forces on IB segment supports due to TFCFD + VDE slow up.

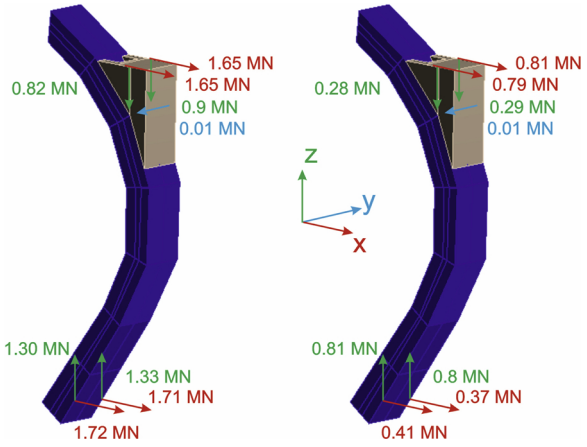

Fig. 10. Reaction forces on COB supports due to TFCFD + VDE slow up.

5.1.1. Ferromagnetic force

The ferromagnetic force on the segments is a static radial force of ~7-8 MN/segment. This force pushes the IB segments against the VV wall and is distributed to its eight radial support pads. The OB segments are pushed in the same direction towards the machine centre and hence off the VV wall. In their case the ferromagnetic force is reacted at the bottom and the top of the segments [3].

Table 3
Reaction forces due to load during normal operation [MN].

IBL				IBR			OBC				OBL				OBR		
Support name	Fx	Fy	Fz	Fx	Fy	Fz	Support name	Fx	Fy	Fz	Support name	Fx	Fy	Fz	Fx	Fy	Fz
Inb. top left	1.92	0.00	−0.01	1.89	0.00	−0.01	Outb. top left	1.60	0.00	−0.71	Outb. top left	1.36	0.00	−0.21	2.12	0.00	−1.99
Inb. top right	1.89	0.00	−0.01	1.92	0.00	−0.01	Outb. top right	1.71	0.00	−1.02	Outb. top right	1.99	0.00	−1.78	1.22	−0.01	−0.01
Inb. high mid`	0.00	0.00	0.00	0.00	0.00	0.00											
Inb. high left	0.43	0.00	0.00	0.40	0.00	0.00											
Inb. high right	0.39	0.00	0.00	0.42	0.00	0.00											
Inb. mid left	0.00	0.00	0.00	0.00	0.00	0.00	Outb. tor OBL	0.00	0.00	0.00	Outb. tor VV-BLK	0.00	0.00	0.00	0.00	0.00	0.00
Inb. mid right	0.00	0.00	0.00	0.00	0.00	0.00	Outb. tor OBR	0.00	−0.08	0.00	Outb. tor BLK-OBC	0.00	0.00	0.00	0.00	−0.08	0.00
Inb. low mid	0.00	0.00	0.00	0.00	0.00	0.00	Outb. bot mid	0.00	0.08	0.00	Outb. bot mid	0.00	0.01	0.00	0.00	0.08	0.00
Inb. bot left	1.39	0.00	0.29	1.25	0.00	0.34	Outb. bot left	1.89	0.00	1.71	Outb. bot left	1.45	0.00	0.91	1.66	0.00	1.29
Inb. bot right	1.25	0.00	0.34	1.40	0.00	0.29	Outb. bot right	1.54	0.00	0.91	Outb. bot right	1.90	0.00	1.92	1.70	0.00	1.54
TOTAL	7.27	0.00	0.61	7.27	0.00	0.61	TOTAL	6.74	−0.01	0.90	TOTAL	6.70	0.00	0.83	6.69	0.00	0.84

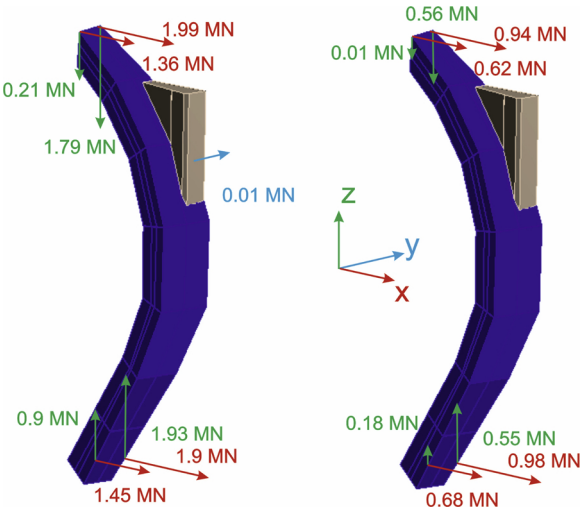

Fig. 11. Reaction forces on LOB supports due to TFCFD + VDE slow up.

5.1.2. EM loads

Severe net EM loads on the BB segments occur due to a major disruption, a TFCFD, or a VDE slow up, see Table 2. The TFCFD load case was found particularly critical in terms of reaction forces: on the inboard segment radial forces add up. The radial force of 8.5 MN due to the TFCFD acts in addition to the ferromagnetic force (~7-8 MN). Due to a slow upward VDE an additional radial force acts on the upper part of each inboard segments of ~4 MN.

On the outboard segments the TFCFD force acts in opposite direction to the ferromagnetic force and hence in a direction in which the blanket is not supported. It needs to be verified that the outboard segments are not pushed off their supports.

The reaction force results for normal operation (Table 3) and the TFCFD + VDE slow up (Table 7) are also illustrated on Fig. 9 (IB left), Fig. 10 (COB) and Fig. 11 (LOB).

5.2. Deformation

The vertical and radial displacements during operation (Fig. 12) show that the outboard segments tend to straighten due to the radial

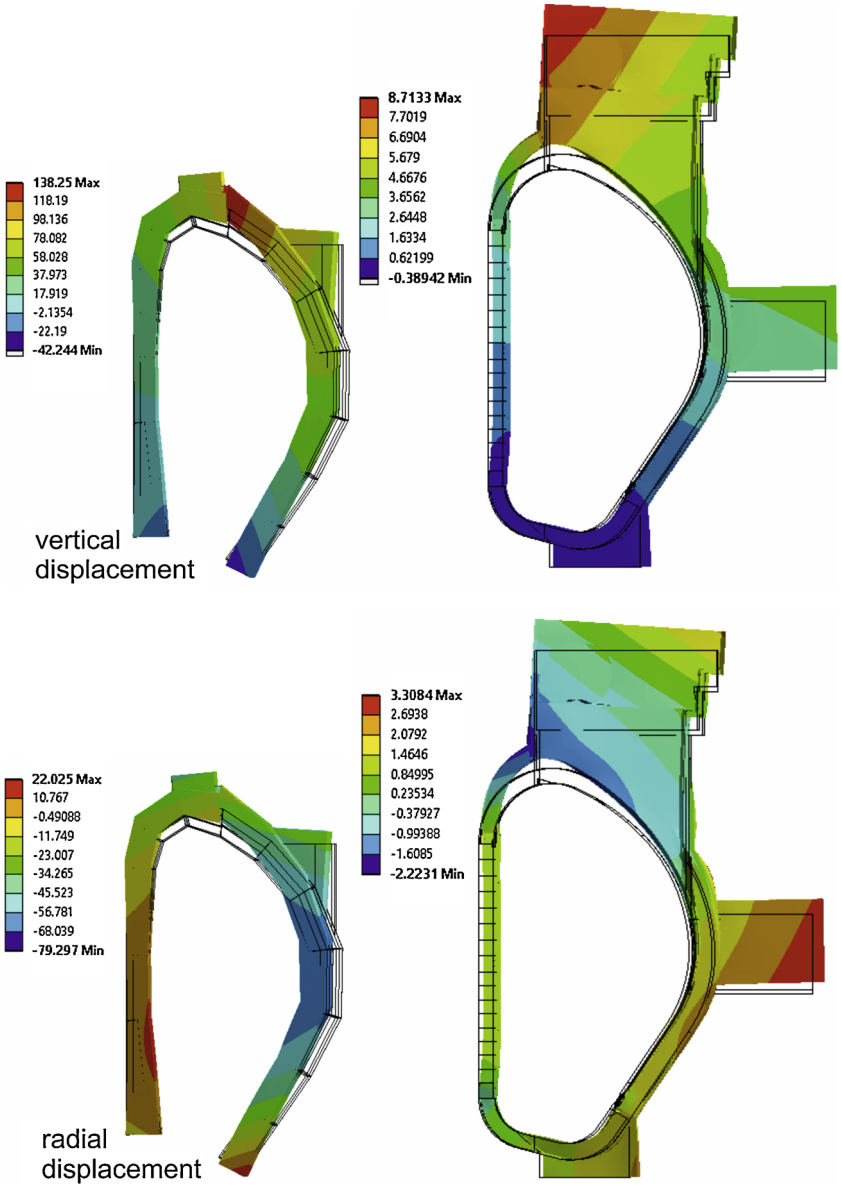

Fig. 12. Vertical (top) and radial (bottom) displacements of segments and vacuum vessel during normal operation [mm].

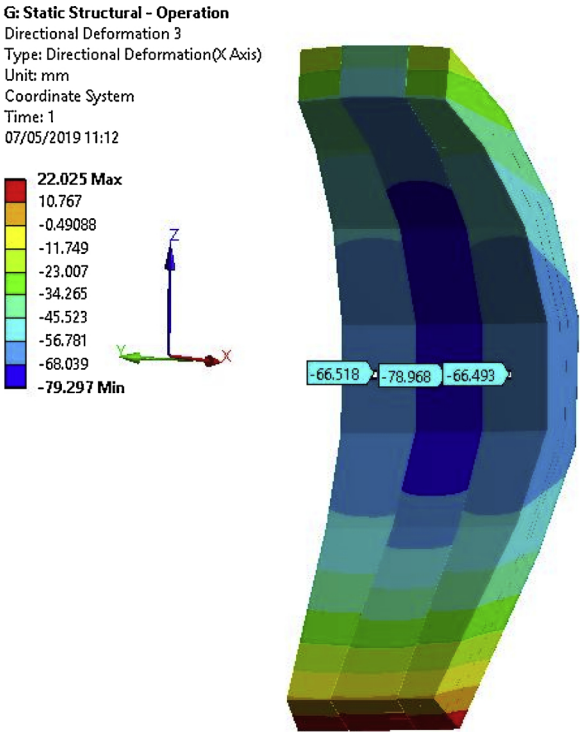

Fig. 13. Radial displacements during normal operation, with values at the centre [mm].

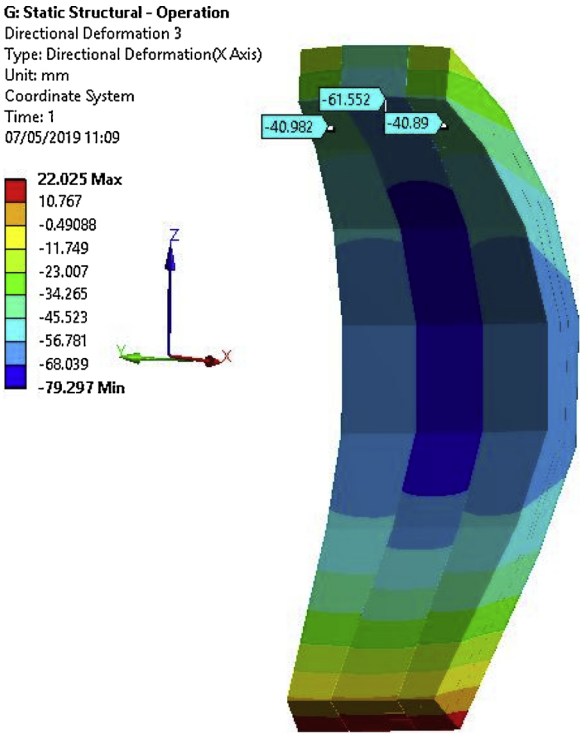

Fig. 14. Radial displacements during normal operation, with values at the top [mm].

temperature gradient in the BB and the radial ferromagnetic force. Similar but less distinct behaviour can be observed on the inboard segment.

The plot of radial displacement during normal operation of the outboard segments (Figs. 13, 14) shows the difference between the central outboard segment and the lateral segments due to the attachment of the COB being further out. The radial displacement difference is ~12 mm in the middle, at the top however it is ~20 mm, although the whole reason of supporting the COB differently is the planned upper limiter, which will be a separate component. The radial displacement difference may be controlled with the initial gaps defined accordingly.

It is also important to note, that despite the reaction forces are asymmetric (Table 3–8) the displacements are symmetric indicating that the displacement differences limited to the local connections between the segments and the VV. Some of the potential reasons of the asymmetries have been identified (i.e.: non-symmetric equatorial port location, lateral outboard segments support on the top), they have not been fully understood. These asymmetries in the reaction forces are not considered to be critical, however the impact of asymmetries in the BB segments, their supports, and their loads will be investigated in the future.

In the tables those reaction force components that need most attention are highlighted; during operation the radial and vertical force components at the bottom and the top of the segments, ex-vessel LOCA the vertical components due to the increased thermal expansion, TFCFD, VDE and TFCFD + VDE the mostly the change in the radial force components and in case of a major disruption the asymmetry in the forces and the toroidal force components due to the moments from the Lorentz forces.

The average blanket displacements at the top and the average vertical upward force against the VV during flat top operation on the top are listed in Fig. 15 for different gap sizes at assembly. This figure shows that the inboard segment is stiff, whereas the outboard segment has sufficient flexibility to prevent over-loading of the supports.

6. Summary

The DEMO blanket attachment concept relies on the radial static magnetic forces similar to an arch bridge support [13].

This concept has been verified for the critical load cases. The reaction forces due to selected off normal events at the blanket attachment points and overall displacements of the blanket segments have been presented using a shell element-based model, which considers gaps and unidirectional constraints. Initial gaps at the top of the blanket segments have been chosen to minimise the thermal stresses in the blanket segments. These details need further refinement and optimisation to make sure that requirements regarding RM and FW alignment are also satisfied. The initial gaps are expected to close during pre-pulse warm-up due to the BB inlet temperature and the ferromagnetic force. At the same time during normal operation or ex-vessel LOCA the reaction forces should remain at tolerable magnitudes. However, due to the stiffness of the inboard segments snap-through components are under consideration in the upper port to prevent excessive reaction forces during ex-vessel LOCA.

Initial studies indicate that up to 3 − 4 MN can be transferred at a single attachment location. However, this may be further limited by the VV or the blanket segment strength.

Based on this, the reaction forces seem to be high in three cases:

- In the TFCFD + VDE slow up case the reaction forces at the inboard at “high” location exceed 4 MN on one side (average reaction force between left and right ~3.5 MN), however either further refinement in the high position, distributing the load between “mid” and “high” or splitting “high” into two locations or achieving symmetrical load distribution between the left and right pads of “high” would bring this force under 4 MN.
- In the case of ex-vessel LOCA there are reaction forces over 4 MN, but this is a result of a very asymmetric load distribution (average reaction force between left and right ~2.5 MN). Either with changing the reaction position, or refining the initial gap sizes, this can be reduced to tolerable levels.

Table 4
Reaction forces due to load during ex-vessel LOCA [MN].

IBL				IBR			OBC				OBL				OBR		
Support name	Fx	Fy	Fz	Fx	Fy	Fz	Support name	Fx	Fy	Fz	Support name	Fx	Fy	Fz	Fx	Fy	Fz
Inb. top left	1.18	0.00	−3.09	0.79	0.00	−0.24	Outb. top left	0.57	0.00	−1.60	Outb. top left	0.55	−0.01	−0.74	1.27	0.00	−4.60
Inb. top right	0.72	0.00	−0.66	1.37	0.00	−2.69	Outb. top right	0.56	0.00	−1.65	Outb. top right	1.27	0.00	−4.58	0.55	0.00	−0.74
Inb. high mid	0.00	0.57	0.00	0.00	0.64	0.00											
Inb. high left	0.00	0.00	0.00	0.00	0.00	0.00											
Inb. high right	0.00	0.00	0.00	0.00	0.00	0.00											
Inb. mid left	−0.01	0.00	0.00	−0.01	0.00	0.00	Outb. tor OBL	0.00	0.00	0.00	Outb. tor VV-BLK	0.00	0.00	0.00	0.00	0.00	0.00
Inb. mid right	−0.01	0.00	0.00	−0.01	0.00	0.00	Outb. tor OBR	0.00	0.00	0.00	Outb. tor BLK-OBC	0.00	0.00	0.00	0.00	0.00	0.00
Inb. low mid	0.00	−0.10	0.00	0.00	−0.13	0.00	Outb. bot mid	0.00	0.00	0.00	Outb. bot mid	0.00	0.35	0.00	0.00	0.35	0.00
Inb. bot left	2.49	0.00	2.07	1.33	0.00	1.81	Outb. bot left	0.97	0.00	2.06	Outb. bot left	0.88	0.00	3.92	0.01	0.00	2.14
Inb. bot right	1.31	0.00	2.29	2.79	0.00	1.73	Outb. bot right	0.98	0.00	2.09	Outb. bot right	0.01	0.00	2.24	0.88	0.00	4.04
TOTAL	**5.67**	**0.47**	**0.61**	**6.26**	**0.51**	**0.61**	**TOTAL**	**3.09**	**0.00**	**0.90**	**TOTAL**	**2.71**	**0.34**	**0.83**	**2.71**	**0.35**	**0.84**

Table 5
Reaction forces due to load during TF coil fast discharge [MN].

IBL				IBR			OBC				OBL				OBR		
Support name	Fx	Fy	Fz	Fx	Fy	Fz	Support name	Fx	Fy	Fz	Support name	Fx	Fy	Fz	Fx	Fy	Fz
Inb. top left	2.18	0.00	−0.74	2.24	0.00	−0.01	Outb. top left	1.04	0.00	−0.36	Outb. top left	0.86	0.00	−0.01	1.36	0.00	−0.99
Inb. top right	2.26	0.00	−0.01	2.16	0.00	−0.74	Outb. top right	1.13	0.00	−0.58	Outb. top right	1.28	0.00	−0.97	0.78	0.00	−0.01
Inb. high mid	0.00	0.04	0.00	0.00	0.04	0.00											
Inb. high left	3.04	0.00	0.00	2.22	0.00	0.00											
Inb. high right	2.16	0.00	0.00	3.02	0.00	0.00											
Inb. mid left	0.01	0.00	0.00	0.05	0.00	0.00	Outb. tor OBL	0.00	0.00	0.00	Outb. tor VV-BLK	0.00	0.00	0.00	0.00	0.00	0.00
Inb. mid right	0.09	0.00	0.00	0.01	0.00	0.00	Outb. tor OBR	0.00	−0.06	0.00	Outb. tor BLK-OBC	0.00	0.00	0.00	0.00	−0.06	0.00
Inb. low mid	0.00	0.04	0.00	0.00	0.04	0.00	Outb. bot mid	0.00	0.06	0.00	Outb. bot mid	0.00	0.00	0.00	0.00	0.05	0.00
Inb. bot left	2.02	0.00	0.00	2.12	0.00	0.00	Outb. bot left	1.26	0.00	1.21	Outb. bot left	0.96	0.00	0.58	1.16	0.00	0.77
Inb. bot right	2.10	0.00	0.00	2.01	0.00	0.00	Outb. bot right	1.00	0.00	0.62	Outb. bot right	1.32	0.00	1.23	1.12	0.00	1.06
TOTAL	**13.85**	**0.08**	**-0.75**	**13.83**	**0.08**	**-0.75**	**TOTAL**	**4.42**	**0.00**	**0.90**	**TOTAL**	**4.43**	**0.00**	**0.83**	**4.42**	**-0.01**	**0.84**

Table 6
Reaction forces due to load during VDE slow up [MN].

IBL				IBR			OBC				OBL				OBR		
Support name	**Fx**	Fy	Fz	Fx	Fy	Fz	Support name	Fx	Fy	Fz	Support name	Fx	Fy	Fz	Fx	Fy	Fz
Inb. top left	1.90	0.00	−1.64	1.98	0.00	−0.31	Outb. top left	1.33	0.00	−0.49	Outb. top left	1.13	0.00	−0.04	1.75	0.00	−1.60
Inb. top right	1.99	0.00	−0.30	1.88	0.00	−1.63	Outb. top right	1.43	0.00	−0.76	Outb. top right	1.64	0.00	−1.54	1.01	0.00	−0.01
Inb. high mid	0.00	0.07	0.00	0.00	0.07	0.00											
Inb. high left	1.93	0.00	0.00	1.51	0.00	0.00											
Inb. high right	1.50	0.00	0.00	1.92	0.00	0.00											
Inb. mid left	0.00	0.00	0.00	0.00	0.00	0.00	Outb. tor OBL	0.00	0.00	0.00	Outb. tor VV-BLK	0.00	0.00	0.00	0.00	0.00	0.00
Inb. mid right	0.01	0.00	0.00	0.00	0.00	0.00	Outb. tor OBR	0.00	−0.07	0.00	Outb. tor BLK-OBC	0.00	0.00	0.00	0.00	−0.07	0.00
Inb. low mid	0.00	0.07	0.00	0.00	0.07	0.00	Outb. bot mid	0.00	0.07	0.00	Outb. bot mid	0.00	0.01	0.00	0.00	0.07	0.00
Inb. bot left	1.59	0.00	0.00	1.70	0.00	0.00	Outb. bot left	1.54	0.00	1.08	Outb. bot left	1.17	0.00	0.40	1.36	0.00	0.76
Inb. bot right	1.70	0.00	0.00	1.60	0.00	0.00	Outb. bot right	1.23	0.00	0.38	Outb. bot right	1.57	0.00	1.35	1.37	0.00	1.01
TOTAL	**10.62**	**0.15**	**-1.94**	**10.59**	**0.15**	**-1.95**	**TOTAL**	**5.52**	**-0.01**	**0.21**	**TOTAL**	**5.51**	**0.00**	**0.16**	**5.50**	**0.00**	**0.16**

Table 7
Reaction forces due to load during simultaneous TF coil fast discharge VDE slow up [MN].

IBL				IBR			OBC				OBL				OBR		
Support name	Fx	Fy	Fz	Fx	Fy	Fz	Support name	Fx	Fy	Fz	Support name	Fx	Fy	Fz	Fx	Fy	Fz
Inb. top left	2.13	0.00	−2.26	2.19	0.00	−1.04	Outb. top left	0.76	0.00	−0.20	Outb. top left	0.62	0.00	−0.01	1.00	0.00	−0.57
Inb. top right	2.20	0.00	−1.04	2.12	0.00	−2.26	Outb. top right	0.84	0.00	−0.37	Outb. top right	0.94	0.00	−0.56	0.56	0.00	−0.01
Inb. high mid	0.00	0.06	0.00	0.00	0.06	0.00											
Inb. high left	4.39	0.00	0.00	2.69	0.00	0.00											
Inb. high right	2.60	0.00	0.00	4.36	0.00	0.00											
Inb. mid left	0.01	0.00	0.00	0.95	0.00	0.00	Outb. tor OBL	0.00	0.00	0.00	Outb. tor VV-BLK	0.00	0.00	0.00	0.00	0.00	0.00
Inb. mid right	1.00	0.00	0.00	0.01	0.00	0.00	Outb. tor OBR	0.00	−0.05	0.00	Outb. tor BLK-OBC	0.00	0.00	0.00	0.00	−0.05	0.00
Inb. low mid	0.00	0.06	0.00	0.00	0.06	0.00	Outb. bot mid	0.00	0.05	0.00	Outb. bot mid	0.00	0.00	0.00	0.00	0.04	0.00
Inb. bot left	2.40	0.00	0.00	2.32	0.00	0.00	Outb. bot left	0.90	0.00	0.63	Outb. bot left	0.69	0.00	0.18	0.87	0.00	0.21
Inb. bot right	2.30	0.00	0.00	2.38	0.00	0.00	Outb. bot right	0.70	0.00	0.15	Outb. bot right	0.98	0.00	0.54	0.79	0.00	0.53
TOTAL	**17.02**	**0.11**	**-3.31**	**17.02**	**0.12**	**-3.31**	**TOTAL**	**3.20**	**0.00**	**0.21**	**TOTAL**	**3.23**	**0.00**	**0.16**	**3.22**	**-0.01**	**0.16**

Table 8
Reaction forces due to load during major disruption [MN].

IBL				IBR			OBC				OBL				OBR			
Support name	Fx	Fy	Fz	Fx	Fy	Fz	Support name	Fx	Fy	Fz	Support name	Fx	Fy	Fz	Fx	Fy	Fz	
Inb. top left	2.28	0.00	−0.01	1.24	0.00	−0.01	Outb. top left	1.62	0.00	−0.01	Outb. top left	3.62	−1.09	−0.01	4.59	0.60	−1.96	
Inb. top right	1.30	0.00	−0.75	2.12	0.00	−0.01	Outb. top right	1.78	0.00	−3.13	Outb. top right	0.01	0.01	−2.12	−1.11	−0.77	−0.31	
Inb. high mid	0.00	0.85	0.00	0.00	1.95	0.00												
Inb. high left	1.38	0.00	0.00	0.00	0.00	0.00												
Inb. high right	0.00	0.00	0.00	1.62	0.00	0.00												
Inb. mid left	0.00	0.00	0.00	0.00	0.00	0.00	Outb. tor OBL	0.00	−1.43	0.00	Outb. tor VV-BLK	0.00	−1.63	0.00	0.00	−1.63	0.00	
Inb. mid right	0.00	0.00	0.00	0.00	0.00	0.00	Outb. tor OBR	0.00	0.01	0.00	Outb. tor BLK-OBC	0.00	−1.43	0.00	0.00	0.01	0.00	
Inb. low mid	0.00	0.85	0.00	0.00	1.95	0.00	Outb. bot mid	0.00	1.43	0.00	Outb. bot mid	0.00	−1.30	0.00	0.00	1.36	0.00	
Inb. bot left	2.34	0.00	0.00	0.47	0.00	0.63	Outb. bot left	2.09	0.00	4.04	Outb. bot left	3.10	0.00	2.96	4.07	0.00	3.11	
Inb. bot right	0.39	0.00	1.37	2.25	0.00	0.00	Outb. bot right	1.56	0.00	0.00	Outb. bot right	0.28	0.00	0.00	−0.68	0.00	0.00	
TOTAL	**7.69**	**1.70**	**0.61**	**7.70**	**3.89**	**0.61**	**TOTAL**	**7.05**	**0.01**	**0.90**	**TOTAL**	**7.01**	**-5.44**	**0.83**	**6.87**	**-0.44**	**0.84**	

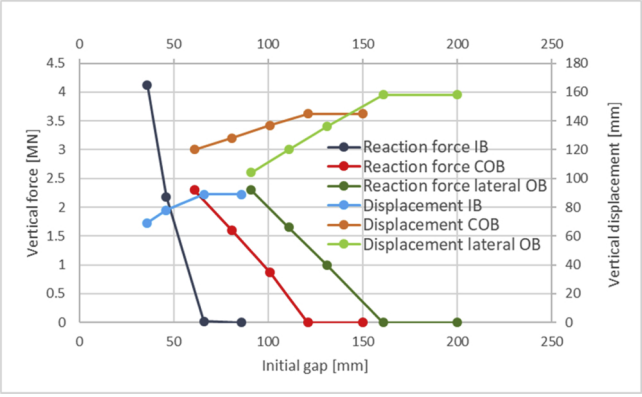

Fig. 15. Effect of initial gap sizes on the vertical reaction forces at the top and the vertical blanket displacements (including VV).

- In the case of major disruption, the analysis indicated that there are high radial forces (in excess of 4 MN) at the lateral blanket segments, however the negative reaction force indicating that the moments due to the eddy currents are twisting these segments so much that they are pushed against the VV. It is also worth to bear in mind that these loads need to be updated for the current baseline.

Further investigation may be necessary to identify the reason in the slight asymmetry observed in the reaction forces.

Thermal expansion of the blanket segments has not yet been comprehensively considered. Various additional thermal states of the segments need to be assessed in the future regarding asymmetric deformation and reaction forces on the supports. The model presented in this work allows future implementation of further components such as limiters to assess their impact as well.

Declaration of Competing Interest

The authors declare that they have no known competing financial interests or personal relationships that could have appeared to influence the work reported in this paper.

Acknowledgments

This work has been carried out within the framework of the EUROfusion Consortium and has received funding from the Euratom research and training programme 2014-2018 and 2019-2020 under grant agreement No 633053. The views and opinions expressed herein do not necessarily reflect those of the European Commission. To obtain further information on the data and models underlying this paper please contact publicationsmanager@ccfe.ac.uk.

References

[1] C. Bachmann, et al., Overview over DEMO design integration challenges and their impact on component design concepts, Fusion Eng. Des. 136 (Part A, November) (2018) 87–95, https://doi.org/10.1016/j.fusengdes.2017.12.040.
[2] R. Mitteau, et al., A shaped first wall for ITER, J. Nucl. Phys. Mater. Sci. Radiat. Appl. 415 (Suppl. 1) (2011) S969–S972.
[3] A.R. Raffray, et al., The ITER blanket system design challenge, Nucl. Eng. 54 (2014) 033004.
[4] C. Bachmann, et al., Initial definition of structural load conditions in DEMO, Fusion Eng. Des. (2017), https://doi.org/10.1016/j.fusengdes.2017.02.061.
[5] F. Hernandez, et al., Overview of the HCPB Research Activities in EUROfusion, (2019).
[6] A. Del Nevo, et al., Recent Progress in Developing a Feasible and Integrated Conceptual Design of the WCLL BB in EUROfusion Project, SOFT, 2018.
[7] C. Vorpahl, Initial Configuration Studies of the Upper Vertical Port of the European DEMO, SOFT, Sicily, Italy, 2018 September 2018.
[8] G. Zhou, F.A. Hernández, C. Zeile, I.A. Maione, Transient thermal analysis and structural assessment of an ex-vessel LOCA event on the EU DEMO HCPB breeding blanket and the attachment system, Fusion Eng. Des. 136 (2018) 34–41, https://doi.org/10.1016/j.fusengdes.2017.12.017.
[9] I.A. Maione, C. Zeile, EUROfusion deliverable BB-9.3.1-T002-D001, EFDA_D_2MXFJL, (2019).
[10] I.A. Maione, EUROfusion deliverable BB-9.3.1-T003-D001, EFDA_D_2N9URR, (2019).
[11] C. Bachmann, Load Specification for the DEMO Vacuum Vessel, EFDA_D_2MBPN6 v.1.8, (2019).
[12] E. Visca, G. Brolatti, P. Frosi, G. Mazzone, Dynamic amplification of blanket load caused by a gap at the supporting key, WP13-DAS02-T08, EFDA_D_2LF84Z, (2019).
[13] C. Bachman, et al., Overview over DEMO design integration challenges and their impact on component design concepts, Fus Eng. Des. 136 (2018) 87–95, https://doi.org/10.1016/j.fusengdes.2017.12.040.